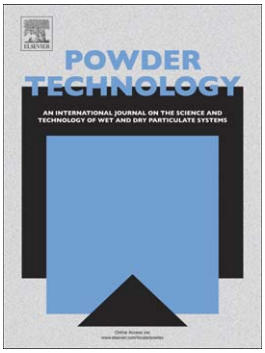

Ammonia-induced precipitation of zirconyl chloride and zirconyl-yttrium chloride solutions under industrially relevant conditions

Geoffrey A. Carter, Mark I. Ogden, Craig E. Buckley, Clinton Maitland, Mark Paskevicius

PII: S0032-5910(08)00269-6
DOI: doi: 10.1016/j.powtec.2008.04.087
Reference: PTEC 7266

To appear in: *Powder Technology*

Received date: 4 March 2008
Revised date: 21 April 2008
Accepted date: 25 April 2008

Please cite this article as: Geoffrey A. Carter, Mark I. Ogden, Craig E. Buckley, Clinton Maitland, Mark Paskevicius, Ammonia-induced precipitation of zirconyl chloride and zirconyl-yttrium chloride solutions under industrially relevant conditions, *Powder Technology* (2008), doi: 10.1016/j.powtec.2008.04.087

Ammonia-induced precipitation of zirconyl chloride and zirconyl-yttrium chloride solutions under industrially relevant conditions.

Geoffrey. A. Carter[a+b], Mark I. Ogden[a*] Craig E. Buckley[b], Clinton Maitland[b] and Mark Paskevicius[b]

[a] AJ Parker Centre for Integrated Hydrometallurgy Solutions, Nanochemistry Research Institute, Curtin University of Technology, PO Box U1987, Perth, Western Australia, 6845, Australia

[b] Centre for Materials Research, Curtin University of Technology, PO Box U1987, Perth, Western Australia, 6845, Australia

Abstract

The influence of concentration and added chloride salts on the solution speciation of zirconyl chloride solutions, and the precipitate formed upon addition of aqueous ammonia, has been investigated. Crystalline zirconium oxychloride octahydrate samples available on an industrial scale were investigated using ICP-OES, XRD and SEM. The samples had a remarkably consistent level of the trace elements and LOI and contained approximately 2 wt.% hafnium. Zirconyl chloride solutions at industrially relevant concentrations of 0.61 and 1.82 M were studied by small angle x-ray scattering, and the particle radii were found to be unchanged within experimental error. Yttrium-zirconium mixed solutions relevant to the Solid Oxide Fuel Cell market (containing 3, 5, 8 and 10 mole% yttrium) were also investigated, and it was found that the added yttrium did not significantly change the particle radii or particle-particle distances.

Solutions at the same concentrations were then precipitated using a continuous double jet precipitation apparatus with aqueous ammonia as the base. Using DLS it was found that the zirconyl chloride solution at higher concentration yielded a larger precipitated particle size (1.0 ± 0.1 μm, 4.2 ± 0.1 μm). The yttrium-zirconium mixed solutions were found to give a consistent increase in particle size with increasing yttrium levels (2.0 ± 0.1 μm, 3.7 ± 0.2 μm, 4.5 ± 0.1 μm and 4.9 ± 0.2 μm). To investigate if the growth effect was most influenced by the cations or the increasing chloride concentrations, sample solutions containing mixtures of caesium chloride / zirconyl chloride and calcium chloride / zirconyl chloride with the same concentration of added chloride anions as that of the 8 mole % yttrium-zirconium sample were precipitated. The increased particle size was found to be most dependent on the type of cation and did not appear to be as significantly dependent on the concentration of chloride ions.

Keywords: zirconia; yttrium; precipitation; small angle x-ray scattering

Corresponding Author current affiliation Nanochemistry Research Institute, Curtin University of Technology, PO Box U1987, Perth, Western Australia, 6845, Australia Tel:- +61 8 9266 2483, Fax:- +61 8 9266 4699 Email:- m.ogden@exchange.curtin.edu.au

1. Introduction

Interest has been growing in zirconium and its behaviour, generated by the increased interest in Solid Oxide Fuel Cells (SOFC). The SOFC in its most basic form is a device for converting hydrogen and oxygen into water with a resulting electrical generation of power. The materials requirements of zirconia for the highly demanding Solid Oxide Fuel Cell (SOFC) market have been outlined in the literature [1, 2]. The current technology for SOFC applications is based around zirconia doped with varying amounts of yttria to give the required crystallographic and mechanical properties required for the respective SOFC design and manufacturing processes [3]. Industrial manufacture of zirconia and zirconia-yttria products can be summarised as a three step operation; (a) hydrolysis of zirconyl chloride and mixing of other solutions, (b) precipitation, (c) calcination [4]. The use of aqueous solutions allows for lower costs of production and reduced waste thus being an industrially attractive way of manufacturing sub-micrometer zirconia and zirconia-yttria composites [5]. A problem with this method is the production of hard agglomerates within the final powder [6-12]. The limited understanding of the fundamental chemistry, particularly during aqueous processing, has complicated attempts to overcome these difficulties. While some control can be achieved through the use of additives such as alcohols and other dispersants [13-15], or controlled hydrolysis using urea [14, 16], for example, these methods are not readily applied to large scale industrial processing. The aim of our work is to improve understanding of the fundamental solution chemistry of the industrial process, and how this relates to the subsequent precipitation processes, and ultimately the properties of the final ceramic product.

The solution structure of zirconyl chloride is dominated by the cyclic tetramer $[Zr_4(OH)_8(OH_2)_{16}]^{8+}$, as determined using techniques such as small-angle X-ray scattering (SAXS), and extended x-ray absorption fine structure (EXAFS) spectroscopy [17, 18]. It has been proposed that these tetramers can condense to form oligomers and eventually colloidal particles of "$Zr(OH)_4$", where the cyclic tetramers are connected by double hydroxy bridges [18]. It has been reported that a further increase in particle size involves aggregation of primary crystallites, based on dynamic light scattering (DLS) experiments in combination with transmission electron microscopy (TEM) [19]. Again condensation reactions involving bridging hydroxyl or oxide species are believed to be involved. In support of this hypothesis, it

has been shown that addition of methanol can inhibit further growth of precipitated particles, presumably by replacing non-bridging hydroxyl groups with methoxy groups, steric hindrance inhibiting further growth [5, 8, 9, 11]. Ethanol has been reported to act in a similar manner to reduce agglomeration and inhibit growth [15]. This is useful when investigating growth of zirconium precipitation as treating the precipitates with alcohol quenches the growth at a given point in time, allowing comparison of the precipitates in relation to input variables .

The monoclinic polymorph is the most thermodynamically stable form of zirconia; a transformation to the tetragonal polymorph occurs at ~1400 K, and then to the cubic phase at ~2700 K [20]. Doping with cations of lower valency, such as yttrium(III), stabilises these high temperature forms, producing materials for use in solid oxide fuel cells as mentioned above [21]. It has been proposed, for an aqueous co-precipitation method, that the yttrium cation substitutes for a zirconium cation in the tetrameric structure, leading to the precipitation of an amorphous solid solution [22]. However, the tetramer structure is reported to be highly kinetically stable, at least under acidic conditions [17]. It is evident that unresolved issues remain and studies are further complicated by the changes in structure that are induced in the subsequent sintering stages [6].

The precipitate that is formed from most solutions containing zirconium by the addition of a base is described as a gelatinous white to clear amorphous product and is generally assumed to be $ZrO(OH)_2$, but may also be $Zr(OH)_4$ [23, 24]. The equation for the precipitation upon increasing the pH with aqueous ammonia can be considered to be;

$$ZrO^{2+} + 2Cl^{-} + 2NH_4OH \Leftrightarrow ZrO(OH)_2 + 2NH_4Cl$$

Many authors assume a specific composition for the precipitate, but as Kirby [25] articulates, zirconium hydroxide is a poorly defined material and is typically closer in structure to hydrated oxide, where the degree of hydration is dependent on many factors [24, 26-29]. Elison and Petrov [27] suggest that when solutions containing mostly Zr^{4+}, which is predominantly present in hot strong acids (> 1 M HCl), are precipitated the resulting material is closer to $Zr(OH)_4$ in composition. In comparison, in weakly acidic solutions (≅ 0.01 M), where the Zr is present in its hydrolysed polymeric form, the precipitate compositions are closer to $ZrO(OH)_2$.

These early studies also showed that solution composition influenced particle size of the precipitate. For example, Britton's electrometric studies of the precipitation of hydroxides found that the Cl to Zr ratio appeared to influence the size of the precipitates [26]. Here we report the influence of concentration and added chloride salts on the solution speciation of zirconyl chloride solutions, and the precipitate formed upon addition of aqueous ammonia.

2. Experimental Procedure

2.1. Samples

Samples of $ZrOCl_2.8H_2O$ crystals from 20 one tonne bulk bags were supplied by Doral Specialty Chemicals (Rockingham, Western Australia). The supplied $ZrOCl_2.8H_2O$ was analysed for trace element levels using Inductive Coupled Plasma Optical Emission Spectroscopy (ICP-OES). The samples were also analysed for their Loss On Ignition (LOI) and ZrO_2 content.

Solutions of 100 g/L and 200 g/L of ZrO_2 (0.81 M and 1.62 M of $ZrOCl_2$) were made from zirconyl chloride crystals dissolved with milli-q water by allowing them to stand for 10 days. The samples used in the solutions came from sample bags 1, 2 and 16. These were chosen as samples representative of those with no trace elements evident (sample 16) and those with the main trace elements present. Sample 1 contained 10 ppm Al whilst sample 2 contained 20 ppm of Na and S.

Yttrium chloride was made by reacting HCl with yttria in a 1:3 stoichiometric ratio then diluting with milli-q water to a concentration of 100 g/l for the oxide. This solution was added to the zirconyl chloride solution to give 3, 5, 8 and 10 mole %.

Both the caesium chloride and calcium chloride solutions were made from solid chloride salts and milli-q water to match the concentration of the yttrium chloride solution. The solutions were added to the zirconyl chloride to give the same total Cl ion concentration as that of the 8 mol%, yttrium-zirconium mixture.

The ammonia solution was 28% AR grade.

2.2. Solution Mixing

All solutions were aged for 10 days prior to use. Solutions were mixed to achieve the desired final compositions at least 24 hours prior to use and left under agitation for that period using a standard laboratory magnetic stirrer and PTFE coated bar.

2.3. Small Angle X-ray Scattering

The small angle scattering technique was employed using the NanoSTAR SAXS instrument at Curtin University of Technology. Two sample detector distances of 65.0 and 22.8 cm were used in order to provide structural information over a wide q-range (where $q = 4\pi\sin\theta/\lambda$ is the scattering vector, 2θ is the scattering angle, and $\lambda = 1.5418$ Å (Cu K_α) is the wavelength of incident radiation). The 2-dimensional detector system allowed for the detection of any anisotropy in the scattering pattern.

The SAXS sample solutions were contained within sealed glass capillaries with an external diameter of 0.5 mm and a wall thickness of 0.01 mm where the listed wall thickness variation was 0.01 mm. A long collection time of 18 hours was used for each sample in order to increase the signal to noise ratio of the scattering pattern. A milli-q water sample (also in a 0.5 mm glass capillary) was used for the subtraction of the background scattering pattern. The raw 2-dimensional data files were background subtracted, and since they only displayed isotropic scattering were radially averaged over 360° in order to provide 1-dimensional data sets of the scattered intensity I and the scattering vector q. These data sets were then converted so that their scattered intensities were on an absolute scale. This was achieved using the method outlined by Buckley *et al.* [30], using a highly cross-linked polyethylene S-2907 standard (from Oak Ridge National Laboratories) with a collection time of 3 hours.

The SAXS data was analysed using the Irena 2 SAS modelling macros [31] in the software package Igor Pro 5 (Wavemetrics, Oregon USA). The Irena macros contain a fitting package which utilises the UFM developed by Beaucage [32-34]. The UFM is especially useful for modelling the present system because it is such a generalised scattering model. The scattering model can be customised to include the scattering from any number of structural levels which exist over various q-ranges in

the scattering pattern. Each structural level consists of both a Guinier regime (which describes the size of the particular structure, i.e. the radius of gyration R_g of the particle) and a power-law regime (which describes how that structure is organised, *i.e.* whether it has smooth surfaces or is disordered). The Irena macros also incorporate a hard sphere structure factor that allows for the scattering from particle-particle correlations to be modelled (assuming they are spherical), and the HPMSA structure factor which accounts for the structure of a dispersion of charged colloidal particles (also spherical) of moderate to high densities interacting through a screened coulomb potential [35, 36].

2.4. Precipitation

The system used was developed to approximate a continuous double jet precipitator, a typical industrial system (Figure 1). The injection pumps for both the acid and base feeds were Gilson Minipulse 3 peristaltic pumps. The injection lines were positioned directly above the outer edge of the agitation impeller set 180^{o} from each other. The pH meter was positioned 90° from both the acid inlet and base inlet with the base of the probe in the same plane horizontally as the centre of the impeller. The mixing vessel overflows into a second which contained ethanol to quench the precipitation process.

The feed rate was controlled to give a constant pH of 6 with a variation of 0.5 of a pH point. The value of 6 was used as it was found through experimentation that this point was the easiest point to control the system and it is well above the reported precipitation point of pH 1.86 to 2.79 dependent on the free HCl in the solution [26], as well as being low enough as to be economical in relation to the amount of base required. The flow rate chosen was sufficient to give approximately 1 hour residence time in the first vessel, this varied minimally as the acid addition was controlled to be the same rate for all precipitations, however small variations in the amount of base used to obtain a pH of 6 resulted in some small changes in residence times. The agitator and impeller used were constant throughout the trials, as was the size of the vessels. The speed of agitation was adopted to give a Reynolds number that places the fluid volume well within the turbulent regime.

The pH of the solutions was measured using an ORION model 720A Bench-top pH meter with a Hanna 0406A glass pH electrode. Prior to measurement the instrument was calibrated using pH 7 and 4 buffer solutions it was also checked against a pH 1 buffer solution.

The reaction was commenced using a 50/50 mix by volume of milli-q water and ethanol,in the overflow vessel. The reaction vessel was initially charged with milli-q water that was agitated. The system was allowed to run to equilibrium over a period equal to 4 residence times to allow the system to come to process equilibrium. The overflow vessel was then emptied and replaced, and the system was run for a further 4 residence times. Samples for analysis were then collected from the overflow vessel. Ethanol was added at 10 minute intervals to the overflow vessel so that a relatively constant 20% (by volume) alcohol to solution ratio was maintained.

Insert Figure 1

2.5. Particle Sizing

The particle sizing was determined using a Malvern Zetasizer nano series NANO-ZS instrument and associated proprietary software. Samples for particle sizing were sonicated in a Cole/Palmer 8891 sonic bath for 5 minutes, The refractive index used was that measured using a VEB Carl Zeiss Jena Abbe refractometer Model G, for a 20% alcohol/milli-q water mix.

2.6. Microscopy

Images of particles were obtained using a Philips XL30 Scanning Electron Microscope (SEM). To allow for SEM investigation the solutions of precipitated hydrated zirconia were placed on stubs with carbon tape and allowed to dry under infrared light. Once dry they were carbon coated in a vacuum. Optical microscopy was conducted using a Nikon Eclipse Me600 microscope in reflected light with varying objective lenses

3. Results

3.1. Sample Analysis

The possibility that process variations were caused by trace impurities in the supplied zirconyl chloride was investigated by analysing a number of batches by Inductively Coupled Plasma Optical Emission Spectrometry (ICP-OES) (Table 1). The detectable contaminants were found to be Al, Cr, Fe, Na and S, although all were only present at the limit of detection.

The ICP results indicated that industrially available zirconyl chloride supplied is remarkably consistent and shows that only limited trace elements (in the order of the limits of detection) are present.

Insert Table 1

3.2. SAXS Analysis of Solutions

The impact of solution speciation upon subsequent precipitation processes of zirconyl chloride is not clear from existing literature. In particular, we aimed to determine if the introduction of yttrium resulted in any changes that might impact on the production of hard agglomerates. Johnson and Kraus conducted ultracentrifugation studies on zirconyl chloride and discussed the affects of ageing with the conclusion that ageing increases the degree of polymerization significantly [37], whilst Clearfield suggests that solutions may not have come into equilibrium even after 10 days [23]. As the literature reviewed was inconclusive on the ageing time, 10 days was chosen somewhat arbitrarily as the ageing time with the justification that the significant data collection times used in the SAXS work (18 hours per sample) would be less than 10% of the ageing time. It was envisaged that this would limit the ageing effects during SAXS data collection. It was also assumed that few manufacturers would have solutions standing for greater than 10 days.

Figure 2 shows the background-corrected, absolute scaled SAXS data for the 0.81 M zirconyl chloride solutions and Figure 3 shows the results for the 1.62 M zirconyl chloride solutions. Figure 4 is the data for the zirconyl chloride and yttrium chloride solutions; the concentration of the zirconyl chloride was 0.81 M. The data can be clearly grouped into two classes, based on the solution concentration (0.81 M.

and 1.62 M.). The data displayed in Figure 2 correspond well with that given by Toth *et al.* who reported a peak for a 0.6 M solution of Zr(IV) occurring just below 0.3 $Å^{-1}$ with the peak for a sample of 1 M concentration occurring at approximately 0.35 $Å^{-1}$ [38]. These results correlate with the solutions presented here, where a maximum peak occurs at 0.30 $Å^{-1}$ for a 0.81 M solution and between 0.4 and 0.5 $Å^{-1}$ for the 1.62 M solutions.

Insert Figures 2, 3 and 4

Generally the average Bragg like spacings between domains d_p is determined from $2\pi/q_{max}$, where q_{max} is the value of q for the maximum peak intensity and thus this is the distance between particles [32]. Since several of the peak shapes in our work are a convolution of the Guinier particle size and the correlation between particles, the average radial distance between particles η is determined either from the UFM [32] or the HPMSA (see Supplementary Information for details on the data analysis). The average radial distance between particles η is similar to the Bragg like spacing but relates a circle of radius η that separates each particle. Table 2 contains the relevant structural and chemical information for the solutions analysed by SAXS. A key point that can be extracted from these data is that the particle radius of the solution species is not changing significantly as solution concentration is increased, nor is it changing up on the addition of yttrium chloride. Toth *et al.* investigated solutions with concentrations from 0.035 to 1 M of Zr and concluded that the R_g of the lower concentrations was 4.5 Å ± 0.1 Å with the higher concentrations returning 4.6 Å ± 0.1 Å, consistent with the results reported here [38].

Insert Table 2

It appears that there is no significant change in the solution speciation of zirconyl chloride solutions, at least as reflected by the particle radius, with changes in concentration or addition of yttrium chloride. Our investigations thus moved on to the precipitation step of the process.

3.3. Particle Size

The aim of this section of the work was to determine how solution composition might impact on the precipitation of the zirconyl oxyhydroxide upon addition of base. The experiments were designed to allow the precipitation to proceed for a certain residence time, after which the growth would be quenched by the introduction of ethanol. To assess and confirm the effect of ethanol in quenching the further growth of the particles, precipitation of a sample of 8 mole% yttrium doped zirconyl chloride was carried out with and without added ethanol in the overflow vessel. With the addition of ethanol the precipitate produced was well dispersed and appeared to be suitable for particle sizing even after standing for 24 hours. In the absence of ethanol, a gelatinous cake resulted that was very dense and difficult to remove from the vessel. Only partial dispersion was possible, and optical microscopy showed many 20 to 30 μm spherical particles, in addition to a large number of smaller particles. The particles were soft and readily broken or deformed. These results indicated that the alcohol is acting as suggested in the literature and inhibiting growth and agglomeration [8, 9, 11, 15].

The DLS particle sizing results are given in Table 2. Figure 5 (a) and (b) are examples of the results from the DLS; all results contained single well-defined peaks. The results listed in Table 2 were developed using at least 15 tests on the same sample. To confirm the reproducibility of the test regime five replicates were made of Zr1 and ZrY8, which were found to be consistent within the standard deviation of the analysis.

Insert Figure 5

To support the DLS results optical and electron microscopy was performed to directly determine the size of the particles. Initially, the samples were washed with ethanol, and then resuspended in ethanol and deposited onto a slide for imaging. The samples were found to be hygroscopic, and this was ascribed to residual ammonium chloride, which has poor solubility in ethanol. The washing regime was thus altered to a mixture of 65% methanol, 20% milli-q water, and 15% reacted solution. The filtrate was then re-suspended in ethanol, and spin coated onto a glass slide. These particles were carbon coated and imaged using SEM. Imaging was complicated by the fact that

the particles suffered from some transformation in the beam. The transformation is believed to be dehydration where the hydrated zirconium transforms to zirconia. A low beam current and accelerating voltage with large spot size and working distance was required, resulting in less than ideal images (Figure S1). Nevertheless, it was possible to use the measurement facilities of the XL30 SEM software to determine the size of the particles. The particle sizes were found to be, on average, 20-30% smaller than those measured by DLS. This is not unexpected, since the particles may have dehydrated to some extent upon isolation, and the DLS measures the hydrodynamic radius of the particles.

In Table 2 it is evident that increasing the zirconyl chloride concentration has a dramatic effect, doubling of the concentration (0.81 M to 1.62 M) results in a four times increase in particle size (1.0 ± 0.1 μm to 4.2 ± 0.1μm). An increase in particle size was expected since the effective supersaturation is higher in the more concentrated solution, leading to increase in growth rate over the residence time of the experiment.

A more remarkable result is the increase in particle size with increasing addition of ytrrium chloride (Table 2). The SAXS results described above suggested that the zirconyl chloride solution species was unchanged with added yttrium chloride, so this increase in precipitated particle size is unlikely to be related to changes in solution speciation. Britton suggested that the Cl to Zr ratio influenced the precipitate size [26]. In addition, an increase in aggregate size with added yttrium chloride has been reported more recently, although without specific comment on the origin of the effect [14]. To investigate if the effect was due to the increased chloride concentration as suggested, a solution of cesium chloride was added to the zirconyl chloride solution and precipitation carried out. The cesium chloride was doped into the zirconyl chloride to give the same overall chloride concentration as that of the sample containing 8 mole % yttrium (ZrY8). The added cesium chloride did result in an increase in the precipitate particle size, however, the increase did not approach that found for the ZrY8 sample (Zr3 ≈ 1.0, ZrCs13 ≈ 1.8 : ZrY8 ≈ 4.5 μm). To further investigate these results, a solution with added calcium chloride was precipitated. This solution was prepared again to match the chloride concentration of both the ZrCs13

and 8 mol.% yttrium samples (ZrY8). The particle size was found to be larger than the ZrCs13 sample but smaller than yttrium sample (ZrCa4 ≈ 2.6 μm). From this it is possible to say that the growth seen in the yttrium doped samples is not entirely due to the change in chloride concentration. This suggests that the cations are taking part in the precipitation process to allow growth of the precipitates and that the charge of the cations influences the particle size. A possible explanation is that the cations are enhancing the coagulation of the initially formed particles, which would suggest that the precipitate surface carries a negative charge. The greater efficacy of the higher charge cations is consistent with this hypothesis, and further investigation is underway to characterise the surface charge of the precipitate.

4. Conclusions

Samples of industrially available crystalline zirconium oxychloride octahydrate were investigated. ICP-OES found that the major trace elements were only present at the limit of detection. SAXS investigation of solutions at two industrially relevant concentrations of zirconyl chloride (0.81 and 1.62 M) suggested that the zirconyl speciation was unchanged. Addition of yttrium chloride also had little effect on the SAXS measurement particle radii.

Precipitation was performed using aqueous ammonia as the base. The precipitate particle sizes were measured by DLS with the 1.62 M solution found to have a significantly larger particle size than the 0.81 M solution (4.2 μm , 1.0 μm). The particle sizes were confirmed by electron microscopy, and were found to be in reasonable agreement. The effect on particle size of adding yttrium chloride was also investigated. Samples of 3, 5, 8 and 10 mole% yttrium-zirconium were found to have increasing particle size with increasing yttrium concentration (2.0, 3.7, 4.5, and 4.9 μm respectively). Experiments were carried out to determine if the change in particle size was predominantly a result of the added cations, or anions. Precipitations were performed with added cesium chloride and calcium chloride, such that the chloride concentration matched that of the 8 mole% yttrium-zirconium solution in each case. The precipitate particles sizes increased with the cation charge (ZrCs13, 1.8 μm; ZrCa4 2.6 μm; ZrY8, 4.5 μm), all being larger than the system with no additives (1.0 μm), despite the fact that the chloride concentration is constant. Thus, it appears from

these data that the particle size increase is dependent on the charge of the added cation, and less so on the chloride concentration.

From this work it is evident that the growth rate of precipitated particles for zirconyl chloride solutions is dependent on the concentration of the starting solution as well as the concentration of added cation and the type of cation present. Controlling these factors may enable optimisation of the precipitate particle size. The impact of added cations on properties such as particle surface charge, and on downstream processing of the zirconia is under investigation.

Acknowledgments:

CB, MO and GC acknowledge the financial support of the Australian Research Council (ARC). GC is the holder of an Australian Postgraduate Award, AINSE Postgraduate award and a Parker Centre Postgraduate Research Award.

References

1. Bellon, O., R. Ratnaraj, and D. Rodrigo, 10YSZ based electrolyte materials for electrolyte supported SOFC's, *5th European SOFC Forum*, 2002.
2. Foger, K. and S.P.S. Badwal, Materials for Solid-Oxide Fuel Cells, Mater. Forum, 21 (1997) 187-224.
3. Ciacchi, F.T., K.M. Crane, and S.P.S. Badwal, Evaluation of Commercial Zicronia Powders for Solid Oxide Fuel-Cells, Solid State Ionics, 73(1-2) (1994) 49-61.
4. Carter, G., R.D. Hart, N.M. Kirby, D. Milosevic, and A.N. Titkov, Chemically-Mixed Powders For Solid Oxide Fuel Cells, J. Australasian Ceram. Soc., 39(2) (2003) 149-153.
5. Jones, S.L. and C.J. Norman, Dehydration of Hydrous Zirconia with Methanol, J. Am. Ceram. Soc., 71(4) (1988) C190-C191.
6. Bannister, M. and W. Garrett, Production of Stabilized Zirconia for use as a Solid-State Electrolyte, Ceramurgia Int., 1(3) (1975) 127-133.
7. Belous, A.G., K.V. Kravchyk, E.V. Pashkova, O. Bohnke, and C. Galven, Influence of the chemical composition on structural properties and electrical conductivity of Y-Ce-ZrO2, Chem. Mater., 19(21) (2007) 5179-5184.
8. Kaliszewski, M.S. and A.H. Heuer, Alcohol Interaction with Zirconia Powders, J. Am. Ceram. Soc., 73(6) (1990) 1504-1509.
9. Lauci, M., Powders Agglomeration Grade in the ZrO2-Y2O3 Coprecipitation Process, Key Eng. Mater., 132-136 (1997) 89-92.
10. Li, W., L. Gao, and J.K. Guo, Synthesis of yttria-stabilized zirconia nanoparticles by heating of alcohol aqueous salt solutions, Nanostruct. Mater., 10(6) (1998) 1043-1049.
11. Rajendran, S., Production of Nano-Crystalline Zirconia Powders and Fabrication of High Strength Ultra-Fine-Grained Ceramics, Mater. Forum, 17 (1993) 333-350.

12. Reed, J.S., *Introduction to the Principles of Ceramic Processing*. 1988, New York: John Wiley and Sons.
13. Li, M.Q., Making spherical zirconia particles from inorganic zirconium aqueous sols, Powder Technol., 137(1-2) (2003) 95-98.
14. Oliveira, A.P. and M.L. Torem, The influence of precipitation variables on zirconia powder synthesis, Powder Technol., 119(2-3) (2001) 181-193.
15. Wang, S.Y., X. Li, Y.C. Zhai, and K.M. Wang, Preparation of homodispersed nano zirconia, Powder Technol., 168(2) (2006) 53-58.
16. Huang, Y.X. and C.J. Guo, Synthesis of Nanosized Zirconia Particles via Urea Hydrolysis, Powder Technol., 72(2) (1992) 101-104.
17. Hagfeldt, C., V. Kessler, and I. Persson, Structure of the hydrated, hydrolysed and solvated zirconium(IV) and hafnium(IV) ions in water and aprotic oxygen donor solvents. A crystallographic, EXAFS spectroscopic and large angle X-ray scattering study, Dalton Trans., (14) (2004) 2142-2151.
18. Southon, P.D., J.R. Bartlett, J.L. Woolfrey, and B. Ben-Nissan, Formation and characterization of an aqueous zirconium hydroxide colloid, Chem. Mater., 14(10) (2002) 4313-4319.
19. Hu, M.Z.C., M.T. Harris, and C.H. Byers, Nucleation and growth for synthesis of nanometric zirconia particles by forced hydrolysis, J. Colloid Interface Sci., 198(1) (1998) 87-99.
20. Fernandez-Garcia, M., A. Martinez-Arias, J.C. Hanson, and J.A. Rodriguez, Nanostructured oxides in chemistry: Characterization and properties, Chem. Rev., 104(9) (2004) 4063-4104.
21. Ormerod, R.M., Solid oxide fuel cells, Chem. Soc. Rev., 32(1) (2003) 17-28.
22. Bokhimi, X., A. Morales, A. Garcia-Ruiz, T.D. Xiao, H. Chen, and P.R. Strutt, Transformation of yttrium-doped hydrated zirconium into tetragonal and cubic nanocrystalline zirconia, J. Solid State Chem., 142(2) (1999) 409-418.
23. Clearfield, A., Structural Aspects of Zirconium Chemistry Review, Pure Appl. Chem., 14 (1964) 91-108.
24. Solovkin, A.S. and S.V. Tsvetkova, The Chemistry of Aqueous Solutions of Zirconium salts (Does The Zirconyl Ion Exist?), Russ. Chem. Rev., 31(11) (1962) 655-669.
25. Kirby, N.M., PhD, *Barium zirconate ceramics for melt processing of barium cuprate superconductors*, 2003, Curtin University of Technology, Perth, Western Australia.
26. Britton, H., Electrometric studies of the precipitation of hydroxides. Part II. The precipitation of the hydroxides of zinc, chromium, beryllium, aluminium, bivalent tin and zirconium by use of the hydrogen electrode, and their alleged amphoteric nature, J. Chem. Soc., Trans., 127 (1925) 2120-2141.
27. Elinson, S.V. and K.I. Petrov, *Analytical Chemistry of Zirconium and Hafnium*. 1969, London: Ann Arbor-Humphrey Science Publishers.
28. Singh, R.P. and N.R. Banerjee, Electrometric Studies on the precipitation of hydrous oxides of some Quadravalent Cations. Part 1. Precipitation of Zirconium Hydroxide from solutions of zirconium salts, J. Indian Chem. Soc., 38(11) (1961) 865-870.
29. Zaitsev, L.M. and G.S. Bochkarev, Peculiarities in the behaviour of zirconyl in solutions, Russ. J. Inorg. Chem., 7(4) (1962) 411-414.
30. Buckley, C.E., C. Maitland, D. Scott, G. Carter, and J. Connolly, Comparison of Specific Surface Area Determined from Small Angle X-ray Scattering (SAXS) and BET, J. Australasian Ceram. Soc., 40(2) (2004) 7-12.

31. Ilavsky, J., *Irena 2 SAS Modelling Macros*. 2005, Advanced Photon Source, Argonne National Laboratory.
32. Beaucage, G., Approximations leading to a unified exponential power-law approach to small-angle scattering, J. Appl. Crystallogr., 28 (1995) 717-728.
33. Beaucage, G. and D.W. Schaefer, Structural Studies of Complex-Systems using Small-Angle Scattering - A Unified Guinier Power-Law Approach, J. Non-Cryst. Solids, 172 (1994) 797-805.
34. Beaucage, G., T.A. Ulibarri, E.P. Black, and D.W. Schaefer, *Multiple Size Scale Structures in Silica-Siloxane Composites Studied by Small-Angle Scattering*, in *Hybrid Organic-Inorganic Composites*. ACS Symposium Series, 1995, p. 97-111.
35. Hansen, J.P. and J.B. Hayter, A Rescaled MSA Structure Factor for Dilute Charged Colloidal Dispersions, Mol. Phys., 46(3) (1982) 651-656.
36. Hayter, J.B. and J. Penfold, An Analytic Structure Factor for Macroion Solutions, Mol. Phys., 42(1) (1981) 109-118.
37. Johnson, J.S. and K.S. Kraus, Hydrolytic Behavior of Metal Ions VI. Ultracentrifugation of Zirconium (IV)and Hafnium (IV) Effect of Acidity on the Degree of Polymerization, J. Am. Chem. Soc., 78 (1956) 3937-3943.
38. Toth, L.M., J.S. Lin, and L.K. Felker, Small-Angle X-ray Scattering from Zirconium(IV) Hydrous Tetramers, J. Phys. Chem., 95(8) (1991) 3106-3108.

Table 1 Trace element levels by ICP-OES and LOI of 20 samples

	Trace element (ppm)										
	Al	Ca	Cr	Fe	Na	Ni	P	S	Si	Ti	Gravimetric (wt.%) LOI
Detection limit	10	20	10	10	20	10	20	20	20	5	
Sample number											
1	10	-	-	-	-	-	-	-	-	-	64.4(1)
2	-	-	-	-	20	-	-	20	-	-	64.8(1)
3	10	-	-	10	-	-	-	-	-	-	63.8(1)
4	-	-	-	10	20	-	-	-	-	-	64.6(1)
5	-	-	-	-	20	-	-	-	-	-	64.4(1)
6	-	-	-	-	20	-	-	-	-	-	61.4(1)
7	-	-	-	10	20	-	-	20	-	-	64.0(1)
8	10	-	-	-	20	-	-	-	-	-	65.4(1)
9	-	-	-	-	-	-	-	-	-	-	65.0(2)
10	-	-	-	-	20	-	-	-	-	-	65.6(1)
11	-	-	10	-	20	-	-	-	-	-	64.1(1)
12	10	-	10	-	20	-	-	-	-	-	64.6(1)
13	-	-	10	-	-	-	-	-	-	-	64.6(1)
14	-	-	-	-	-	-	20	-	-	-	67.2(1)
15	-	-	-	-	-	-	-	-	-	-	63.9(1)
16	-	-	-	-	-	-	-	-	-	-	64.5(1)
17	-	-	-	-	-	-	-	-	-	-	64.2(1)
18	-	-	-	-	-	-	-	-	-	-	64.5(1)
19	-	-	-	-	-	-	-	-	-	-	64.0(1)
20	-	-	-	-	-	-	-	-	-	-	66.3(1)

(- denotes less than detectable limits)*.

(Value in brackets denotes the uncertainty in the last decimal place)+

Table 2. Results of SAXS and precipitate particle size analyses, including pH, concentration, radius of gyration R_g (Å), particle radius R (Å), packing factor k and particle to particle interaction distance d_p (Å), and precipitate particle size mean diameter p (μm).

Sample	Conc. (M)	Added Cations	pH	R_g ±0.3 Å	k	R ±0.4 Å	d_p (Å)	p (μm)
Zr1	0.81		0.74	4.4	1.64	5.7	21	1.0(1)
Zr2	0.81		0.74	4.3	1.80	5.6	21	
Zr3	0.81		0.73	4.4	1.62	5.7	21	1.1(1)
Zr4	1.62		0.45	3.9	5.24	5.1	14	
Zr5	1.62		0.46	3.9	3.80	5.1	15	
Zr6	1.62		0.47	4.1	3.70	5.3	16	4.2(1)
ZrY3	0.81	YCl_3 (3 mol%)	0.77	4.3	1.60	5.6	22	2.0(1)
ZrY5	0.81	YCl_3 (5 mol%)	0.76	4.3	1.31	5.6	21	3.7(2)
ZrY8	0.81	YCl_3 (8 mol%)	0.77	4.3	1.70	5.6	22	4.5(1)
ZrY10	0.81	YCl_3 (10 mol%)	0.72	4.3	1.74	5.6	20	4.9(2)
ZrCa4	0.81	$CaCl_2$ (4.2 mol%)	0.76					2.6(1)
ZrCs13	0.81	CsCl (12.7 mol%)	0.76					1.8(1)

Figure Captions

Figure 1 Diagram of precipitation rig used in experimentation

Figure 2. SAXS data after correction for 0.81 M zirconyl chloride samples. The horizontal axis is the scattering vector q in $Å^{-1}$ whilst the vertical axis is the absolute intensities in cm^{-1}.

Figure 3. SAXS data after correction for 1.62 M zirconyl chloride samples.

Figure 4. SAXS data after correction for all yttrium-zirconium mixed samples, from 0 to 10 mole %.

Figure 5 (a) DLS results for 0.81 M precipitates (PS 990 nm), (b) DLS results for ZrY8 precipitates (PS 4480 nm)

Ammonia-induced precipitation of zirconyl chloride and zirconyl-yttrium chloride solutions under industrially relevant conditions. Part 1

Geoffrey. A. Carter, Mark I. Ogden and Craig E. Buckley, Clinton Maitland and Mark Paskevicius

Supporting Information

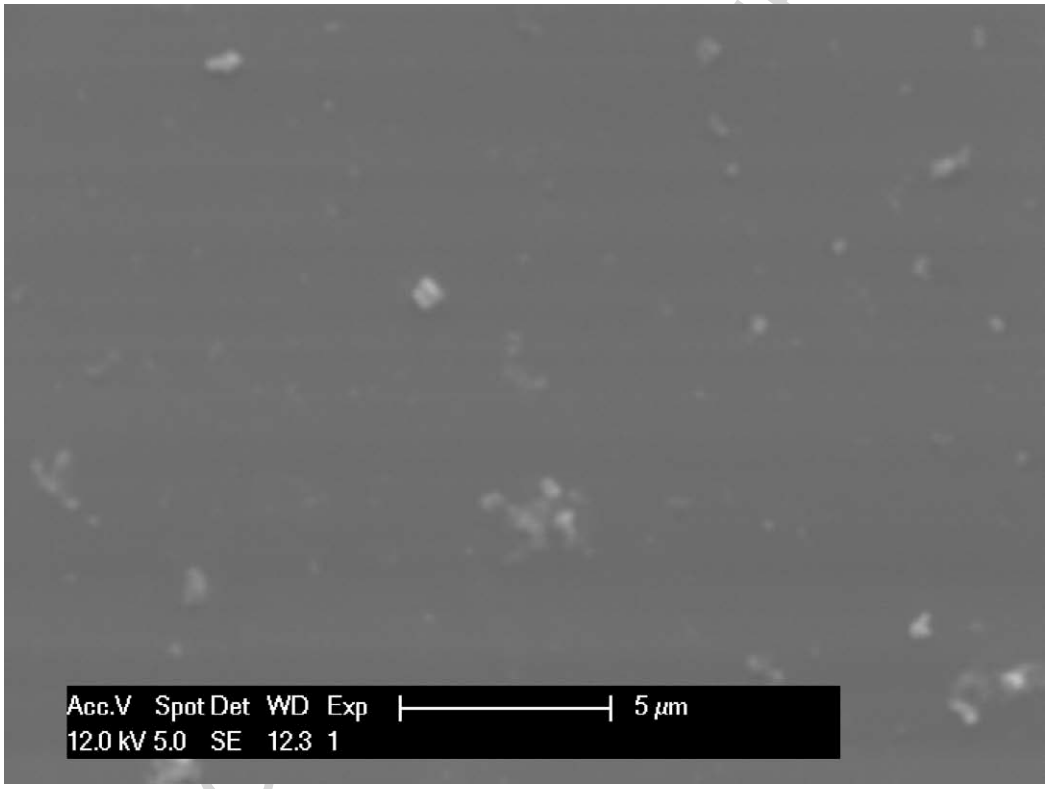

Figure S1 SEM micrograph of spun coated 0.81 M precipitates

Small Angle X-ray Scattering – Data Analysis

The UFM was applied to the data from SAXS for the 0.81 M solutions using Irena. In Irena, the data is fitted using the following model [1],

$$I(q) = I_U(q)S(q) \qquad (1)$$

where $I_U(q)$ is intensity due to the unified model given by

$$I_U(q) \approx G_1 \exp\left(-q^2 R_{g1}^2/3\right) + B_1\left\{\left[\ erf\left(qkR_{g1}/\sqrt{6}\right)\right]^3/q\right\}^{P_1} + \sum_{i=2}^{n}\left(G_i \exp\left(-q^2 R_{gi}^2/3\right) + B_i \exp\left(-q^2 R_{g(i-1)}^2\right)\left\{\left[\ erf\left(qkR_{gi}/\sqrt{6}\right)\right]^3/q\right\}^{P_i}\right) \qquad (2)$$

G_i is the Guinier law prefactor, P_i is the power law, B_i is the power law prefactor, k = 1.06 for mass fractals or k = 1 for every other case, i is the level and $S(q)$ is the structure factor for spherical particles given by

$$S(q) = \frac{1}{1 + k\phi} \quad (3)$$

where $k = 8V_H/V_o$ is the packing factor, V_H is the hard core volume of a domain and V_o is the average volume available to a domain (for face centred Cubic (FCC) packing of spheres $k = 5.92$).

$$\phi = 3\frac{\sin(q\eta) - q\eta\cos(q\eta)}{q^3\eta^3} \quad (4)$$

where η is the average radial distance between particles. Equations 1, 3 & 4 are for weakly correlated systems and for these equations to be applicable the value of k must be less than four [2].

For the 1.62 M solutions the structure factor $S_1(K_1)$ for spherical particles used in the HPMSA model [3] is given by (5)

$$S_1(K_1) = \frac{1}{1 - 24\xi\, a(K_1)} \quad (5)$$

where ξ is the volume fraction and $a(K_1)$ is a dimensionless quantity described in full detail in the literature [3].

Fig. S2 shows the fit to the scattering data achieved using the UFM for the 0.81 M solution (sample Zr1). This is a typical fit to the data for all the 0.81 M solutions measured and represents close agreement between the experimental intensities and that of the model. From Table S2, $k < 4$ for samples Zr1, Zr23 & Zr3, and hence the application of equation (1) is appropriate for these samples. Fig. S3 displays the scattering data for the same starting raw material, with the solution concentration at 1.62 M (sample Zr6). The model doesn't fit as neatly as for the 0.81 M solutions, particularly at low q. From Table S2, $k < 4$ for samples Zr5 & Zr6, but only just (k = 3.8 and 3.7 respectively) and since $k > 4$ for sample Zr4 the criteria to use equation 1 is not satisfied, therefore the HPMSA model was used for the 1.62 M solutions (Fig. S4). The HPMSA model offers a more refined method than the UFM in the case of the 1.62 M solutions as it takes into account the particle to particle interactions using a screened coulomb approach. When the 0.81 M solutions were modelled using the HPMSA the method failed to converge, which makes sense since in general the mean spherical approximation fails at low density [3, 4]. This result coupled with the success of the UFM for the 0.81 M solutions and the success of the HPMSA for the 1.62 M solutions validates the analysis method.

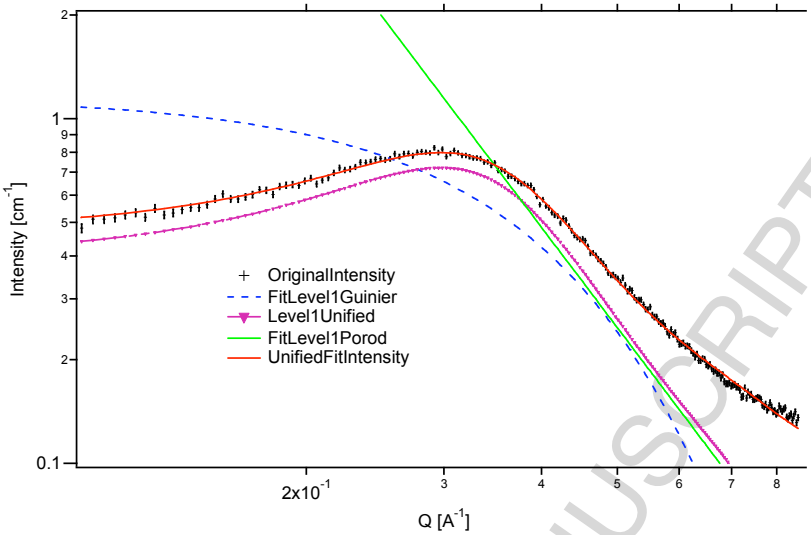

Fig. S2 Data and fitted model for sample Zr1 concentration of 0.81 M. The plot shows the contribution from the Guinier and the power law parts of the UFM equation.

Fig. S5 displays the fit to a similar scattering pattern, for a 0.81 M solution with 8 mol % yttrium-zirconium mixture. Samples ZrY3, ZrY5, ZrY8 & ZrY10 all have values of $k < 4$, therefore η (Table S2) will be a more accurate representation of the average radial particle to particle distance than d_p. The result for all of the 0.81 M solutions, are essentially identical irrespective of yttrium levels.

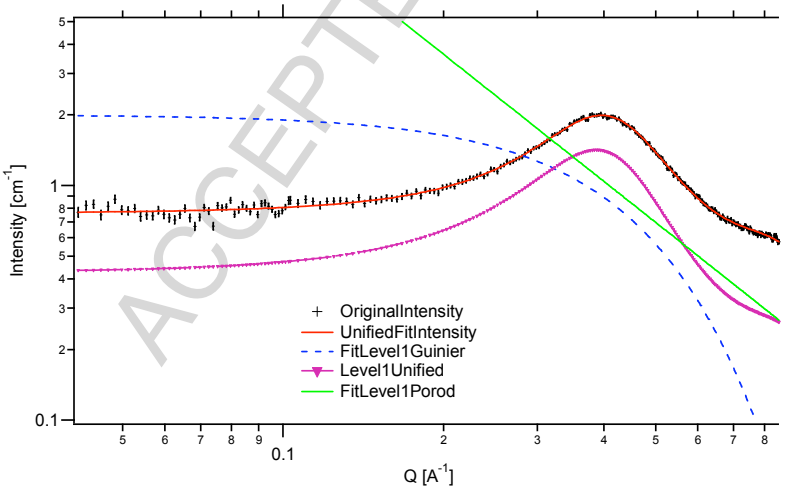

Fig. S3 Data and fitted model using the UFM for sample Zr67, concentration 1.62 M. The plot shows the contribution from the Guinier and the power law parts of the UFM equation.

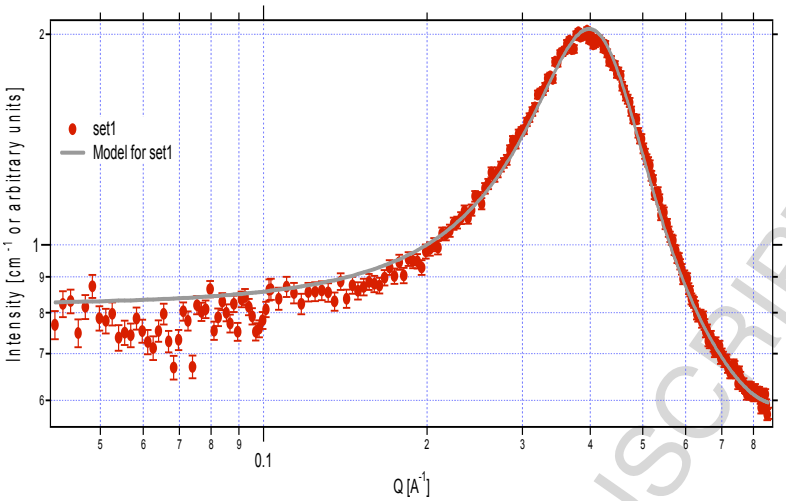

Fig. S4 Data and Fitted model using the HPMSA for sample Zr6, concentration 1.62 M.

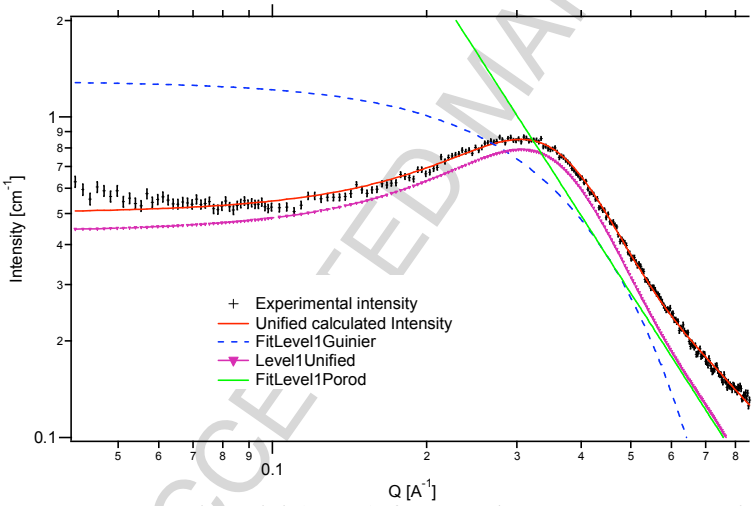

Fig. S5 Data and model (UFM) for sample ZrYy8 concentration 0.81 M with 8 mole % yttrium added. The plot shows the contribution from the Guinier and the power law parts of the UFM equation.

Table S2. Results of SAXS and precipitate particle size analyses, including pH, concentration, radius of gyration R_g (Å), particle radius R (Å), packing factor k and particle to particle interaction distance d_p (Å) and η (Å), and precipitate particle size mean diameter p (μm).

Sample	Conc. (M)	Added Cations	pH	R_g ±0.3 Å	η ±1.0 Å	k	R ±0.4 Å	d_p (Å)	p (μm)
Zr1	0.81		0.74	4.4	16.1	1.64	5.7	21	1.0(1)
Zr2	0.81		0.74	4.3	15.9	1.80	5.6	21	
Zr3	0.81		0.73	4.4	16.0	1.62	5.7	21	1.1(1)
Zr4	1.62		0.45	3.9	14.9	5.24	5.1	14	
Zr5	1.62		0.46	3.9	15.0	3.80	5.1	15	
Zr6	1.62		0.47	4.1	15.2	3.70	5.3	16	4.2(1)
ZrY3	0.81	YCl_3 (3 mol%)	0.77	4.3	16.3	1.60	5.6	22	2.0(1)
ZrY5	0.81	YCl_3 (5 mol%)	0.76	4.3	15.7	1.31	5.6	21	3.7(2)
ZrY	0.81	YCl_3 (8 mol%)	0.77	4.3	15.6	1.70	5.6	22	4.5(1)
ZrY10	0.81	YCl_3 (10 mol%)	0.72	4.3	15.2	1.74	5.6	20	4.9(2)
ZrCa4	0.81	$CaCl_2$ (4.2 mol%)							2.6(1)
ZrCs13	0.81	CsCl (12.7 mol%)							1.8(1)

1. Beaucage, G. and D.W. Schaefer, Structural Studies of Complex-Systems using Small-Angle Scattering - A Unified Guinier Power-Law Approach, J. Non-Cryst. Solids, 172 (1994) 797-805.
2. Beaucage, G., Approximations leading to a unified exponential power-law approach to small-angle scattering, J. Appl. Crystallogr., 28 (1995) 717-728.
3. Hayter, J.B. and J. Penfold, An Analytic Structure Factor for Macroion Solutions, Mol. Phys., 42(1) (1981) 109-118.
4. Hansen, J.P. and J.B. Hayter, A Rescaled MSA Structure Factor for Dilute Charged Colloidal Dispersions, Mol. Phys., 46(3) (1982) 651-656.

Graphical Abstract

Ammonia-induced precipitation of zirconyl chloride and zirconyl-yttrium chloride solutions under industrially relevant conditions.

Geoffrey. A. Carter, Mark I. Ogden and Craig E. Buckley, Clinton Maitland and Mark Paskevicius

The influence of concentration and added chloride salts on the solution speciation of zirconyl chloride solutions, and the precipitate formed upon addition of aqueous ammonia, has been investigated. Solution speciation was not measurably influenced by concentration or added chloride salts, but particle size of the precipitate was found to be dependant on the type and concentration of added cation.